

# Chapter - IV

Studies On D.C. And A.C.  
Electrical Conductivity.

## CHAPTER-IV

### STUDIES ON D.C. AND A.C. ELECTRICAL CONDUCTIVITY

#### 4.1 INTRODUCTION :

Ferrites exhibit semiconducting behaviour. Ferrites have wide range of resistivity. At room temperature resistivity can vary from  $10^{-3}$  ohm-cm to  $10^9$  ohm-cm. High resistivity ferrites are beneficial to use them at high frequencies. Ferrites with high resistivity are widely used for the cores of intermediate and high frequency electromagnetic devices.<sup>1,2</sup> In  $\text{Fe}_3\text{O}_4$ , low resistivity is observed due to the presense of  $\text{Fe}^{2+}$  and  $\text{Fe}^{3+}$  ions in the crystallographically equivalent sites.<sup>3</sup> In ferrites the iron ions with two valance states  $\text{Fe}^{2+}$  and  $\text{Fe}^{3+}$  leads to n-type conductivity<sup>4</sup> by exchange of electrons from donar ion  $\text{Fe}^{2+}$  to  $\text{Fe}^{3+}$  in the same lattice. (octahedral lattice). This requires little energy to move an electron.

The studies on conductivity enables a useful data from application point of view and also in understanding the mechanism of conduction. Conduction in ferrites is attributed to 'electron hopping' model i.e. hopping process in which electrons jumps from one lattice sites to other under the influence of electric field. The conductivity in 'Cu' containing ferrite was explained by Condarache<sup>5</sup> on the basis of hopping process. In ferrite the temperature dependent resistivity is given by,

$$\rho = \rho_0 \exp (\Delta E/kT) \quad \dots(4.1)$$

where  $\rho_0$  = is temperature independent constant which depends on the nature of material.

$k$  = is the Boltzman constant.

$T$  = is the absolute temperature.

$\Delta E$  = is the activation energy.

Komar<sup>6</sup> et al have observed breaks or discontinuities in  $\log \rho$  versus  $1/T$  plots for many ferrites. The discontinuity occurs near Curie temperature and segment represents different conduction mechanisms. The break may also be due to change in the dominant conduction mechanism. Verway<sup>7</sup> et al have observed this type of discontinuities in Mn-Ni ferrite. According to him these discontinuities shifted towards higher temperature as 'Mn' content increases. They observed high activation energy of materials to be due to high resistivity at room temperature. Romejin<sup>8</sup> has observed such discontinuities in  $Mn_3O_4$  and  $Fe_3O_4$  at low temperature.

Van Vlietret<sup>9</sup> has observed the changes in resistivities of 'Ni' sample at room temperature before and after grinding the surfaces in Ni-Zn ferrites. He attributed this change to 'Zn' which volatilizes during heat treatment and encourages the formation of  $Fe^{2+}$  ion on the surface. Due to this, Ni-Zn ferrite shows low resistance before grinding the surface. Koops<sup>10</sup> has studied the variation of resistivity and dielectric constant with frequency. He

found that the resistivity and dielectric constant fall by large amount of higher frequencies in inhomogeneous material.

The 'hopping of polarons' by thermal activation also contributes to the conduction. The existence of small polaron and hopping process was confirmed experimentally.<sup>11</sup> The 'two phase polaron' model<sup>12</sup> is made available (1975) to explain conduction mechanism. The conduction mechanism in ferrites is due to the exchange of electrons in the lattice. Recently Klinger<sup>13</sup> has reviewed the conduction mechanism in ferrites. He stated that the hopping of polarons is the main conduction mechanism in ferrites. Contribution to resistivity of materials are from cation distribution, crystal structure, porosity, grain size, impurity inclusions chemical or oxidation states and other unknown and known scattering mechanisms.

Parker<sup>14</sup> et al have measured resistivity of non stoichiometric Zn and Ni ferrite and observed discontinuities in the resistivity plots. Ahmad<sup>15</sup> et al have observed the discrepancies in the theoretical and observed results. They have measured the temperature dependence of electrical conductivity, Hall effect and thermoelectric power of Cu-Zn ferrites and interpreted the results on the basis of hopping of small polarons. Domain wall resonance in 'Cu' containing ferrites has been studied by Srinivasan<sup>16</sup> and he has attributed this resonance to hopping process.

In this chapter review of the conduction mechanism in oxides and ferrites is given. Polaron theory is briefly discussed.

Experimental details of resistivity, Curie temperature, dielectric measurements are given. The observed results are discussed and attempts has been made to discuss with the present theoretical models.

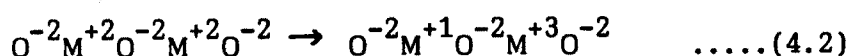
#### 4.2 CONDUCTION MECHANISM :

In general oxide crystal structure may be conveniently regarded in terms of oxygen ions. Although the bonding in the transition metal oxides is predominantly ionic, the electrical conductivity tends to be decided by the electron with d-like wave function and most probably the impurity states.

In the elements of first transition series the 3d levels are being systematically filled from Si to Ni. In the crystalline field of a solid, the levels are splits up into a triplet and doublet. The triplet states lie below the doublet e.g. states in oxides with rock salt structure. These oxides then expected to be metallic conductor at least above antiferromagnetic temperature.<sup>17</sup> Below the Neel temperature the exchange forces could give rise to further splitting of 3d band. The oxide behaves as semiconductor at all temperatures and have intrinsic activation energies in excess of those which could be accounted by exchange of splitting. From this it is evident that the discriptions in terms of conventional band structure fails to account for the electrical transport properties.

#### 4.3 CONDUCTION IN OXIDES :

For an oxide of composition MO, the activation of a conduction electron may be represented by,



where M is divalent transition metal ions.

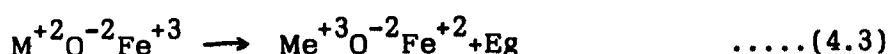
The energy needed for the formation of ion pair ( $M^{+2}M^{-2}$ ) and ( $M^{+3}M^{+1}$ ) corresponds to a gap in the density of states. The following terms are contributed to the activation energy.

1. The difference between ionisation energy and the electron affinity of the free  $M^{+2}$  ion.
2. The difference in modelung energy of the two configuration shown in equation (4.2).
3. The difference in crystal field stabilization energy of the above configuration.
4. Energies of polarisation of the surrounding crystal lattice.

A relatively good conductivity in ionic compounds with an appreciable concentration of metal ions in two valance state was first suggested by De-Boer and Verwey<sup>18</sup> for magnetite. Magnetite has 1/3 of metal ions on tetrahedral sites and 2/3 on an octahedral sites. The process differs from one represented in equation (4.2) and energy term by (4) polarisation effect is only present. The overlap between 3d like wave functions of nearest neighbour cation is sufficient to give metallic type conduction.

#### 4.4 CONDUCTION IN FERRITES :

The above mechanism of electron transport does not apply to other simple ferrites, where all Fe ions are trivalent. The transport may be represented as,



where Eg is activation energy and may reflect the difference between third ionisation potential of  $Fe^{3+}$  and  $M^{+3}$  ions in the solid. Jonker<sup>19</sup> has studied the ferrite  $Co_xFe_{3-x}O_4$  and predicted the mechanism as stated above.

Analogous considerations may apply to cations of mixed valancy in ferrites which results from a departure from the ideal metal to oxygen ratio. An oxygen ion vacancy will contribute two extra electrons to the 3d band. If the extra charges are detached their vacancies by thermal agitation, n-type conductivity is induced in oxygen excess materials. Some oxides are very difficult to prepare homogeneously with stoichiometric anion to cation ratio. Extrinsic semiconduction may then prevail throughout the temperature region amenable to electric measurements. In such cases it may still be possible to infer the activation energy of intrinsic conduction samples from which extrinsic effects have been suppressed by introduction of compensation impurities.

This was first demonstrated by Van-Uitred<sup>20</sup> in  $NiFe_2O_4$  by replacing 1 to 2% Fe by Mn or Co. Electrons donated by oxygen vacancies will fill the impurity levels. Mixed valancy state will be confined to the impurity elements if its local concentration exceeds twice that of oxygen vacancies. This technique is based on the assumption that impurity band conduction is absent and the allowed impurity concentrations indicate that the cation wave function do not extend significantly beyond nearest neighbour distance in the B-lattice.

Electrons and holes are to move by thermally activated hopping mechanism except for pseudometallic composition region close to magnetite.

#### 4.5 CONDUCTIVITY :

Electronic conduction of ferrites can be associated with the presence of ions of given element. In ferrite the conductivity is due to the occurrence of both  $\text{Fe}^{2+}$  and  $\text{Fe}^{3+}$  ions in the spinel structure. The classic example is  $\text{Fe}^{2+}\text{Fe}_2^{+3}\text{O}_4$  one of the non metallic conductor.<sup>21</sup> The presence of  $\text{Fe}^{2+}$  ion will be considered to assure reduced resistivity in ferrite system. To achieve high resistivity it is common practice to avoid an excess of  $\text{Fe}_2\text{O}_3$  and oxidising atmosphere during sintering. The resistivity will also be caused by certain factors which are apart from the inherent properties.

- i. Porosity and porosity is filled by air.
- ii. The grain size of individual crystallite influence the conduction path due to number of grain to grain contact.<sup>22</sup>
- iii. Chemical inhomogeneity caused during preparation or heat treatment.

#### 4.6 ELECTRON HOPPING AND POLARONS :

The electrostatic interaction between a conduction electron or hole and nearest ions may results in the displacement of the latter and hence in polarisation of the surrounding regions. So the carrier becomes situated at the centre of the polarisation potential well. If this well is deep enough a carrier may trapped at a lattice site and its translation to a neighbouring site may be determined by thermal

activation. This has been described by hopping mechanism that the electron takes in a diffusion process by jumps from one lattice site to another. The expression for mobility<sup>23</sup> can be written as,

$$\mu = e^2 d^2 \gamma / kT \exp(-E/kT) \dots\dots(4.4)$$

where  $d$  = is the distance between nearest neighbours.

$\gamma$  = frequency of vibration of lattice.

$E$  = activation energy for hopping process.

with development of polaron theory it becomes evident that the equation (4.4) represents a special case of much more complicated relation between mobility ( $\mu$ ) and a parameter of ionic lattice.

For the calculation of mobility a knowledge of approximate spatial extent of the potential well is required. If the potential well extends over many lattice unit in the crystal, the excess charge may be considered to interact with a dielectric continuum and this model has been employed by Frohlich<sup>24</sup> to formulation interaction Hamiltonian for large polarons. For small polarons the well is confined to a volume comparable to the ionic volume. The actual polaron size can be inferred from consideration of the free energy. Small polaron formulation is favoured in solids which combine a large coupling constant with narrow conduction band. At low temperature a small polaron behaves as a particle moving in a very narrow band. At high temperature small polaron motion may results from the absorption of one or more phonons and this process is essentially the hopping mechanism. If the time of tunnelling of the excess charge from one

ion to the next ion is less, then small polaron conduction will be dominant transport mechanism. There is strong experimental evidence for the existence of small polarons and for the hopping process.<sup>25</sup>

#### 4.7 THERMOELECTRIC POWER :

Studies on thermoelectric power provides a method to separate the contribution to activation energy  $E$  in the expression (4.5).

$$\sigma = B/T \exp ( q_1+q_2+E)/kT) \quad \dots\dots(4.5)$$

For the electrical conductivity assuming the schematic band structure model<sup>26</sup> for the oxide semiconductor. The phenomenological relation between the Peltier coefficient and the Seebeck coefficient together with equation of electrical conductivity in terms of carrier concentration and their mobility gives the relation.

$$eQ = - K \log ( N'_0/n) \quad \text{for n type} \quad \dots\dots(4.6)$$

$$eQ = K \log( N'_0/n) \quad \text{for p type} \quad \dots\dots(4.7)$$

Studies on this gives the density of charge carriers and their average mobility together with electrical conductivity measurements.

#### 4.8 KOOP'S THEORY :

In case of ferrite material the dielectric constant and resistivity are frequency dependent. To explain this type of abnormal behaviour Koops<sup>27</sup> gave a phenomenological theory which is based on simple model. According to Koop the measured capacitance ( $C_p$ ) and parallel resistance ( $R_p$ ) of the specimen results from the equivalent circuit shown in Fig. (4.1). In the Figure (4.1a)  $C_1, C_2, R_1$  and  $R_2$  are all constant but the quantities ' $C_p$ ' and ' $R_D$ ' in Fig. 4.1(b) are

not shows a frequency dependance. A sintered ferrite material is not homogeneous. It may be supposed that the grains of ferrites are moderately good conductor. The inhomogeneous structure is not unlike that discussed by Maxwell<sup>28</sup> and Wagner<sup>29</sup>. This is represented most simply as a double layer dielectric as shown in Fig.(4.2) where subscript 2 refers to the ferrite grains and 1 as the boundary layer. Considering the specimen as a parallel plate capacitor of plate area A, then Koop's Theory

$$C_1 = \epsilon_0 \epsilon_1 A/d_1, \quad C_2 = \epsilon_0 \epsilon_2 A/d_2 \quad \dots\dots(4.8)$$

$$R_1 = \rho_1 d_1/A, \quad R_2 = \rho_2 d_2/A \quad \dots\dots(4.9)$$

where  $\epsilon_0 \epsilon$  = is permittivity and

$\rho_1, \rho_2$  = are resistivity

Then it is followed by equating the impedances in the representation of Fig. 4.1(a) and 4.1(b) that,

$$\beta_p = \rho_p^\infty + \rho_p^0 - \rho_p^\infty / (1 + \omega^2 \tau_p^2) \quad \dots\dots(4.10)$$

and,

$$\epsilon_p = \epsilon_p^\infty + (\epsilon_p^0 - \epsilon_p^\infty) / (1 + \omega^2 \tau_\epsilon^2) \quad \dots\dots(4.11)$$

The suffix 'p' denotes the equivalent parallel representation and the subscripts ' $\infty$ ' and 'o' refers to very high frequency and very low frequency values respectively. The  $\tau_s'$  are relaxation constant and  $\omega = 2\pi\gamma$  where,

$\gamma$  = is measuring frequency.

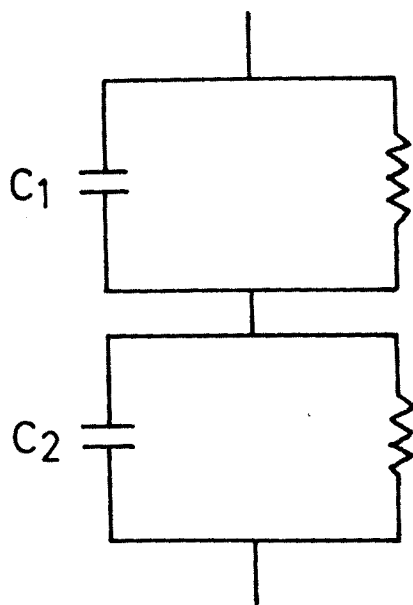


Fig. 4.1 (a)

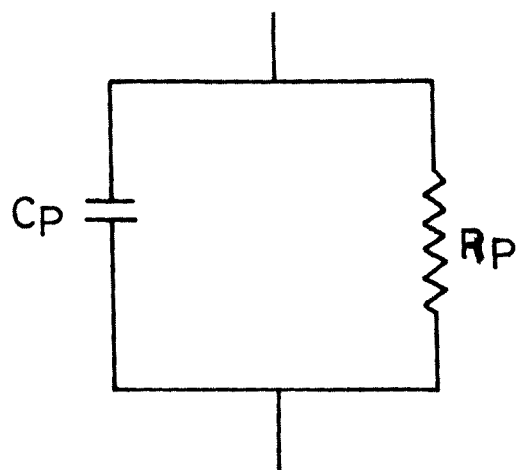


Fig. 4.1 (b)

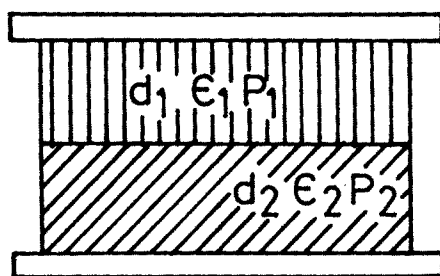


Fig. 4.2

Koop made the following further assumption.

i)  $X = \rho_1 / \rho_2 \ll 1,$

and

ii)  $\rho_1 \gg \rho_2$

iii) Although X is small,  $X \rho_1 \gg \rho_2$  by reasonable factor.

iv)  $\epsilon_1 = \epsilon_2$  for most of the oxides.

Then we found that,

$$\rho_p = \rho_2 + (X \rho_1 / (1 + b \rho_1 \rho_2 \omega^2 / X)) \dots (4.12)$$

and

$$\epsilon_p = \epsilon_2 + (\epsilon_2 / X) / (1 + b \rho_2^2 \omega^2 / X^2) \dots (4.13)$$

where b is constant

At very high frequencies

$$\rho_p^\infty = \rho_2 \text{ and } \epsilon_p^\infty = \epsilon_2 \dots (4.14)$$

At very low frequencies

$$\rho_p^0 = \rho_2 + X \rho_1 \text{ and } \epsilon_p^0 = \epsilon_2 + (\epsilon_1 / X) \dots (4.15)$$

Thus in order to obtain the values of  $\epsilon$  and  $\rho$ , the measurement should be extended and extra-polated to high frequencies.

Koop found the values of 'x' of the order of 0.01 and low frequency dielectric constants is of the order of  $10^4$  or  $10^5$  were found. The above theory would suggest an effective boundary layer of only a few A.U. thick. If the losses in capacitor are represented

by a complex dielectric constant  $\epsilon = \epsilon_p - i \epsilon''$  instead of a parallel resistance, then it follows that,

$$\epsilon'' = 1.16 \times 10^{11} / \omega \rho_p \quad \dots\dots(4.16)$$

where  $\rho_p$  is in ohm-cm.

Bady and Collins<sup>30</sup> measured both the dielectric constant and loss tangent ( $\tan \delta$ ) of number of ferrites over the range of temperature of 25°C to 250°C. the dielectric constant generally increased by not more than 300 parts per million per °C,  $\tan \delta$  also generally increases with temperature. The resistivity of the oxide materials itself is not expected to be frequency dependent. Further at moderately low frequencies in high apparent dielectric constant material the dimensional resonance may occur. The approximate wavelength inside the specimen is given by,

$$\lambda = C / (\mu_i \epsilon_p)^{1/2} \quad \dots\dots(4.17)$$

where  $\mu_i$  is initial permeability at frequency  $\gamma$ , and C be the velocity of free space.

Brockman<sup>31</sup> et al found the values of  $\epsilon_p$  about  $10^4$  and  $\mu_i$  about  $10^3$  in Mn-Zn ferrite, resulting in serious losses for a specimen having dimension of 2cm at a frequency of 2.5 MHz because of the same reason.

#### 4.9 EXPERIMENTS :

##### 4.9 (a) CONDUCTIVITY CELL AND MEASUREMENT OF D.C. RESISTIVITY :

The block diagram of the conductivity cell is as shown in

Fig. 4.3. It consists of two cylindrical brass rods which are fitted in two porcelain discs. The porcelain discs can be held firmly by connecting rods with the help of nuts so as to sandwich the sample between the two cylindrical rod. The electrically insulated Cu-wires were used for external connections.

Initially silver paste was applied on the surface of pellet and then pellet was sandwiched in between two brass rod. The conductivity cell, thus prepared was placed in a temperature regulated furnace. The calibrated chromel-Alumel thermocouple was used to measure the temperature. A circuit diagram for the measurement of d.c. resistivity is as shown in Fig. 4.4. The D.C. electric field was provided from regulated power supply unit (Aplab model 7111) about 5 volts. The current was measured with the help of digital multimeter. The resistivity with temperature of the mixed ferrite series  $\text{Cd}_{0.3}\text{Ni}_{0.7+t}\text{Mn}_t\text{Fe}_{2-2t}\text{O}_4$  ( $t= 0$  to  $0.4$ ) were made from room temperature to  $600^\circ\text{C}$  at an interval of  $25^\circ\text{C}$ . The resistivity ( $\rho$ ) was calculated by using the relation.

$$\rho = \pi r^2/t \quad V/I \quad \dots\dots(4.18)$$

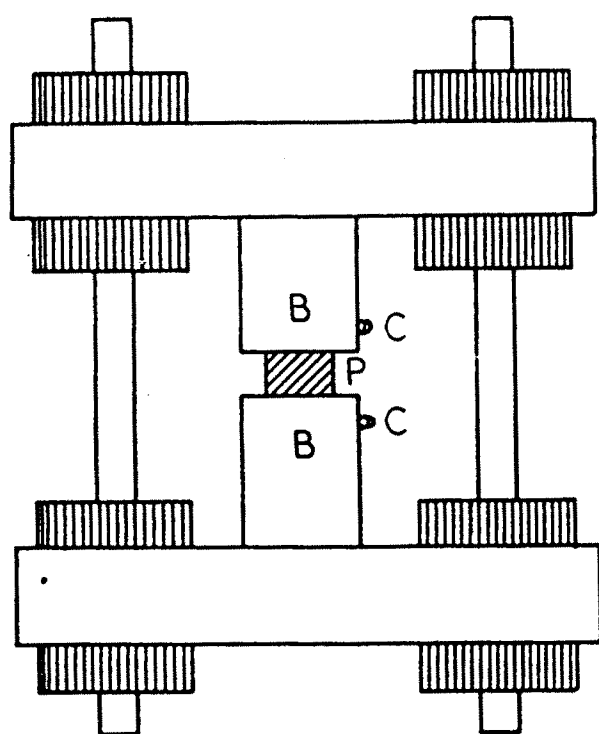
where  $t$  = is the thickness of the pellet in cm.

$r$  = is radius of the pellet in cm

$I$  = is the current in ampere.

#### 4.9 (b) A.C. CONDUCTIVITY MEASUREMENT

The measurement of dielectric constant and loss tangent ( $D = 1/Q = \tan\delta$ ) was carried out at E.T.D.C. Bangalore, on L.C.R bridge (Hewlett Paackard model -4192 A) The frequency range was used from 100Hz to 10MHz. All the measurements were made at room



P - Pellet  
 B - Brass electrode  
 C - Connection lead

Fig. 4.3

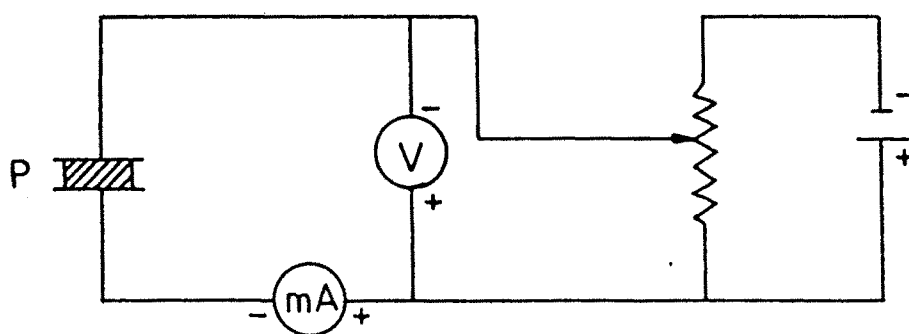


Fig. 4.4 Sample holder and circuit diagram for electrical resistivity

temperature. The samples were used in the form of pellet. These pellets were pasted with silver for good contacts. The pellets were kept in the sample holder firmly. From the observations dielectric constants were calculated by using the relation,

$$\epsilon' = C d / \epsilon_0 A \quad \dots(4.19)$$

where, C = is capacitance in farad.

d = is the thickness of the pellet in cm.

A = area of the pellet.

$\epsilon_0$  = is constant of permittivity

$$= 8.85 \times 10^{-12} \text{ m.k.s unit.}$$

The complex permittivity were calculated by using the relation as,

$$D = 1/Q = \tan \delta = \epsilon'' / \epsilon' \quad \dots(4.20)$$

#### 4.10 RESULTS AND DISCUSSION :

##### 4.10(a) D.C. RESISTIVITY :

The variation of  $\log \rho$  versus temperature are plotted in Fig. 4.5, 4.6. The figure exhibits linear relationship throughout the temperature range suggesting that the resistivity obeys the Arrhenius relationship.

$$\rho = \rho_0 \exp (\Delta E/kT) \quad \dots(4.21)$$

where  $\rho_0$  = is temperature independent constant

k = is Boltzman constant,

t = is absolute temperature.

$\Delta E$  = is the activation energy.

The activation energy is calculated from these plots and are reported in Table 4.1

**TABLE 4.1**  
**VALUES OF ACTIVATION ENERGY (eV)**

Composition	Activation energy eV		
	I region	II region	III region
$\text{Cd}_{0.3}\text{Ni}_{0.7}\text{Fe}_2\text{O}_4$	0.3425	0.4966	0.4513
$\text{Cd}_{0.3}\text{Ni}_{0.75}\text{Mn}_{0.05}\text{Fe}_{1.9}\text{O}_4$	0.3642	0.6456	0.4966
$\text{Cd}_{0.3}\text{Ni}_{0.8}\text{Mn}_{0.1}\text{Fe}_{1.8}\text{O}_4$	0.4966	0.6953	0.9029
$\text{Cd}_{0.3}\text{Ni}_{0.85}\text{Mn}_{0.15}\text{Fe}_{1.7}\text{O}_4$	0.3565	0.4966	1.1919
$\text{Cd}_{0.3}\text{Ni}_{0.9}\text{Mn}_{0.2}\text{Fe}_{1.6}\text{O}_4$	0.3902	0.5959	0.4583
$\text{Cd}_{0.3}\text{Ni}_{1.0}\text{Mn}_{0.3}\text{Fe}_{1.4}\text{O}_4$	0.3104	0.4966	0.7449
$\text{Cd}_{0.3}\text{Ni}_{1.1}\text{Mn}_{0.4}\text{Fe}_{1.2}\text{O}_4$	0.3973	0.5959	0.7773

The resistivity plots shows three distinct regions and two breaks. The temperature  $T_1$  corresponds to transition from region I to II and temperature  $T_2$  from region II to III. The transition temperature ' $T_2$ ' is nearly equal to the Curie temperature of the samples. (Indicated in Fig. 4.5, 4.6).

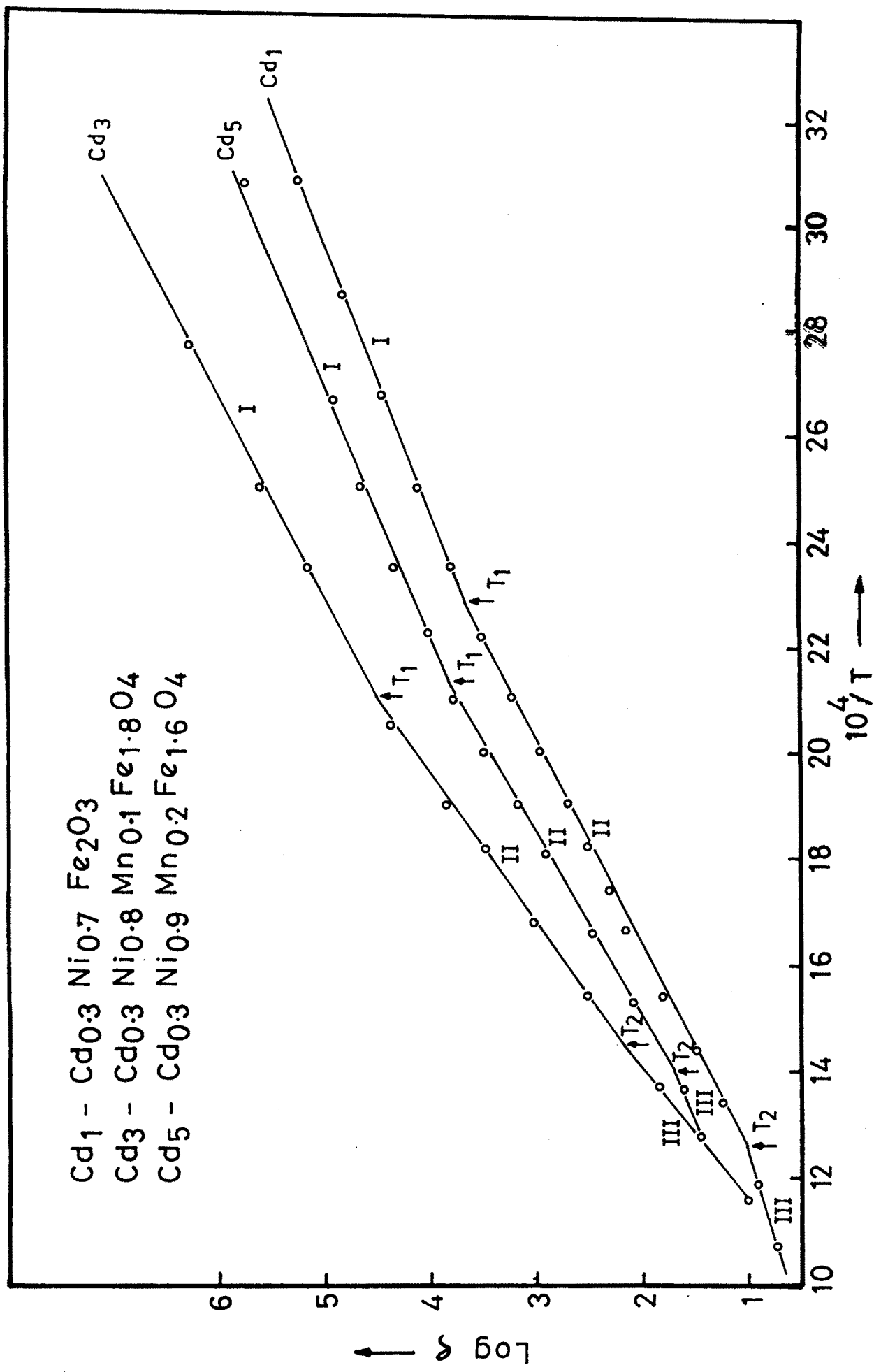


Fig. 4.5 - Variation of  $\log \epsilon$  vs  $10^4/T$ .

Cd2 - Cd0.3 Ni0.75 Mn0.05 Fe1.9 O4  
 Cd6 - Cd0.3 Ni1.0 Mn0.8 Fe1.4 O4  
 Cd7 - Cd0.3 Ni1.0 Mn0.4 Fe1.2 O4

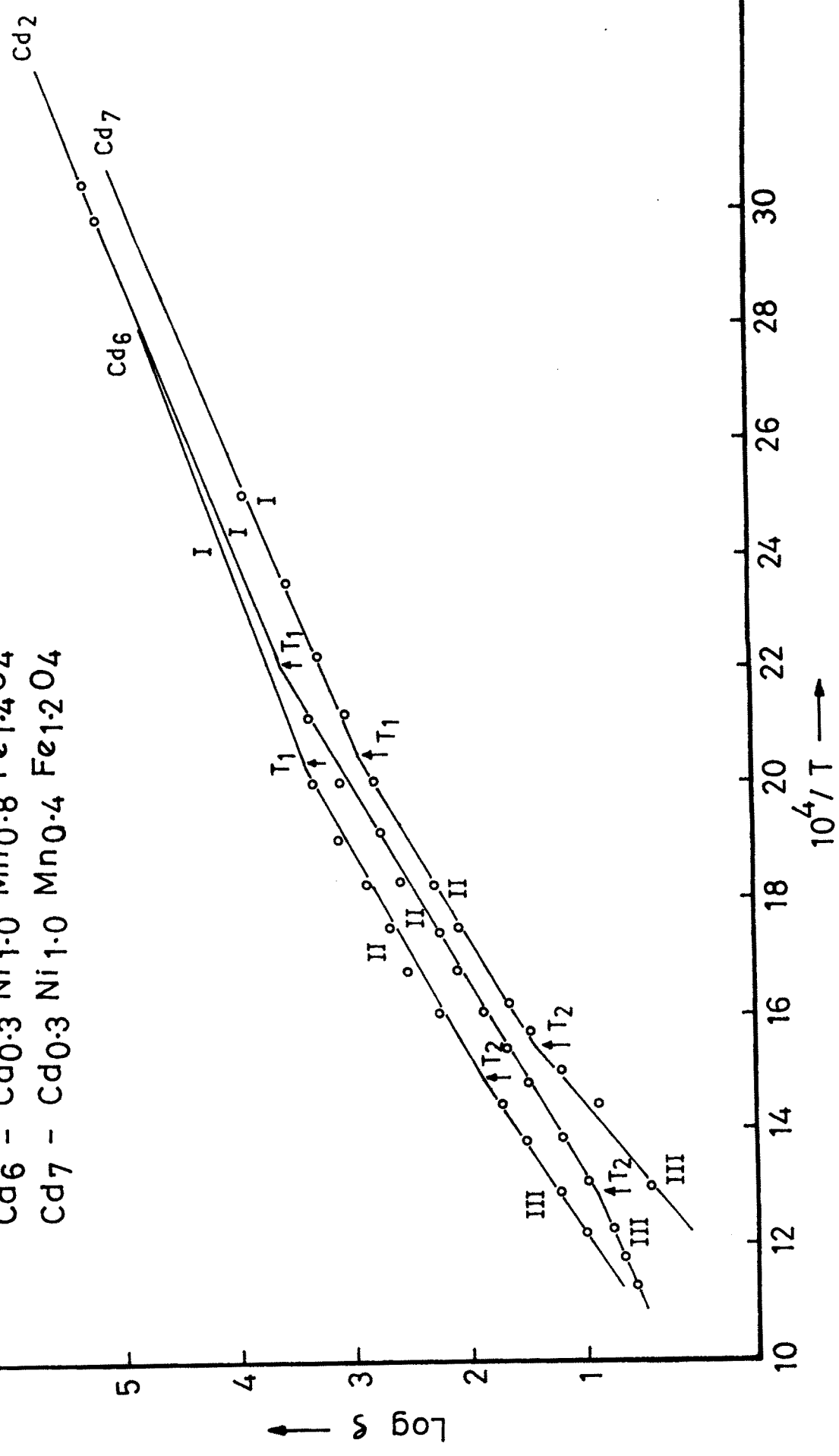


Fig. 4-6 - Variation of  $\log S$  vs  $10^4/T$ .

Komar and Klivshin<sup>32</sup> have observed the changes in the conductivity plots near Curie temperature. Verwey<sup>33</sup> et al have showed, this type discontinuity in Mn-Zn ferrites and these discontinuities shifted with respect to Mn contents. They also observed high activation energy of the material to be due to high resistivity of the materials at room temperature. Ghani<sup>34</sup> et al have observed three regions in the temperature variation of resistivity in Cu-Ni ferrites. They attributed the conduction mechanism in the first region to the presence of impurities, second region to the phase transition and third region to magnetic disorder. From the Table 4.1 It is clearly observed that the  $\Delta E$  values are smaller in region I than in region II and III for all the samples. The low values of  $\Delta E$  in the region I means less activation energy for the conduction of electrons. This may well be attributed to conduction due to impurities which is generally observed in ferrites at low temperatures.

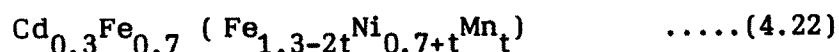
The variation of D.C. resistivity with temperature can be attributed to ionic drift current, current due to electron hopping and current due to electrons in the conduction bands. The current due to ionic drift is known to increase the resistivity with an increase in temperature, where as current due to an electron hopping and electrons in the conduction band results in a decrease of resistivity. The observed variation of resistivity with temperature in the first region may be due to compensation of ionic drift current and current due to electron hopping. The second and third region are characterised due to electron hopping. The anomalous behaviour was observed in

Sn and Zn substituted Ni ferrites.<sup>35</sup>

The conductivity in ferrites has been associated with the presence of ions of given element in more than one valance state and these ions get distributed over the crystallographically equivalent sites e.g. the high conductivity of  $\text{Fe}_3\text{O}_4$  has been explained as transistion of  $\text{Fe}^{3+}$  to  $\text{Fe}^{2+}$  and reverse. The values of ' $\Delta E$ ' to cause normal electron hopping are of the order of 0.2eV and less. The high values of ' $E$ ' for our samples suggest that the hopping process due to polarons is favoured. Mostly in ferrites, the conduction mechanism is explained on the basis of hopping of polaron due to thermal activation.

Ferrites having the spinel structure the B-B distances are smaller than A-A and A-B distances, even the B-B distance is much larger than the sum of ionic radii of cations, indicating little or no overlap between d-wave function of ions on adjacent octahedral site. This gives rise to situation in which the electrons are not free to move through crystal, but remain fixed on B-site necessiating a hopping process. The results of this by hopping process is large effective mass and low mobility of charge carriers. In our case the conduction can possibly be attributed to electron hopping between  $\text{Fe}^{2+} \rightarrow \text{Fe}^{3+}$ ,  $\text{Ni}^{2+} \rightarrow \text{Ni}^{3+}$ ,  $\text{Fe}^{2+} + \text{Mn}^{3+} \rightarrow \text{Fe}^{3+} + \text{Mn}^{2+}$ ,  $\text{Ni}^{3+} + \text{Mn}^{2+} \rightarrow \text{Ni}^{2+} + \text{Mn}^{3+}$ . such ions can be formed during the preparation which are mainly depend on the sintering condition and substituting elements.

For the present system the cation distribution is given by,



The A-A hopping may not exist as there are only  $\text{Fe}^{3+}$  ions and any  $\text{Fe}^{2+}$  formed during preparation, preferentially occupies the B-site. Therefore B-B hopping is more predominant. Thus reduction of  $\text{Fe}^{3+}$  ions on addition of  $\text{Mn}^{4+}$  formation of  $\text{Mn}^{3+}$  and  $\text{Ni}^{3+}$  at higher concentrations of Mn are responsible to change the resistivity behaviour.

Addition of ions with incomplete 3d and 4s shells like  $\text{Sc}^{3+}$ ,  $\text{Ti}^{4+}$  and  $\text{V}^{5+}$  usually leads to an increase in resistivity.<sup>36</sup> They act as electrostatic traps for the exchange of electrons between  $\text{Fe}^{2+}$  and  $\text{Fe}^{3+}$  ions. When they are at octahedral sites, they can also act as scattering centers. These effects lead to an increase in resistivity. The resistivities are expected to increase due to localization of  $\text{Fe}^{2+}$  on addition of  $\text{Mn}^{4+}$  and overall decrease of  $\text{Fe}^{3+}$  hence the increase of resistivity.

Electrical conduction in our samples may be due to the exchange of electrons between  $\text{Mn}^{3+}$  and  $\text{Mn}^{4+}$  ions. Such exchange gives rise to an interesting trapping effect due to local Jahn-Teller distortions around  $\text{Mn}^{3+}$  ions. Around a  $\text{Mn}^{3+}$  ion ( $d^4$  electronic configuration) the six oxygen ions are not equidistant from the central ion, the two being at a larger distance than the rest four. On the other hand, the six oxygen ions around a  $\text{Mn}^{4+}$  ion ( $d^3$  configuration) are equidistant from the central ion. In such a case, when an electron jumps from a  $\text{Mn}^{3+}$  ion to the neighbouring  $\text{Mn}^{4+}$  ion, the new  $\text{Mn}^{4+}$  ion formed at the old site

of the  $Mn^{3+}$  will be surrounded by the tetragonally distorted octahedron of the oxygen ion. Similarly the new  $Mn^{3+}$  will be surrounded by the cubic octahedron of the oxygen ions. Both these arrangement are energetically unstable and a rearrangement of the oxygen jump is associated with the movement of a large number of oxygen ions. This makes the movement of electron from one site to another more difficult and leads to a Jahn-Teller trapping. This would give rise to an additional activation energy for the mobility. This type of behaviour of resistivity is seen in copper magnetite, studied by Sabane<sup>37</sup> et al.

The electrical properties of Mn-Zn ferrites were studied by r.K. Puri et al.<sup>38</sup> According to their observations, as the concentration of Mn ion increases,  $Fe^{3+}$  ions start migrating from octahedral to tetrahedral sites. It increases hopping of electrons in tetrahedral sites and this decreases the resistivity. It is also suggested that the conduction can possibly be attributed to exchange of electrons between  $Fe^{2+} \rightarrow Fe^{3+}$ ,  $Ni^{2+} \rightarrow Ni^{3+}$  and  $Mn^{2+} \rightarrow Mn^{3+}$  ions. since our samples were sintered in air and during cooling process oxidation and reduction of iron ions are possible and above processes may be responsible for the decrease in resistivity.

The Fig 4.7, 4.8 shows the variation of resistivity and activation energy with 'Mn' content. It is observed that the resistivity and activation energy shows one to one correspondance. The resistivity increases upto 0.1 of 'Mn' content and decreases with increase of 'Mn' content. Considering the above facts the increase in resistivity is due to the formation of stable bonds of Mn with Fe at B-site, localization effect and Jahn-Teller trapping. The decrease in resistivity at higher temperatures can be attributed to the formation of  $Ni^{3+}$  and  $Mn^{3+}$  which changes the cation distribution.

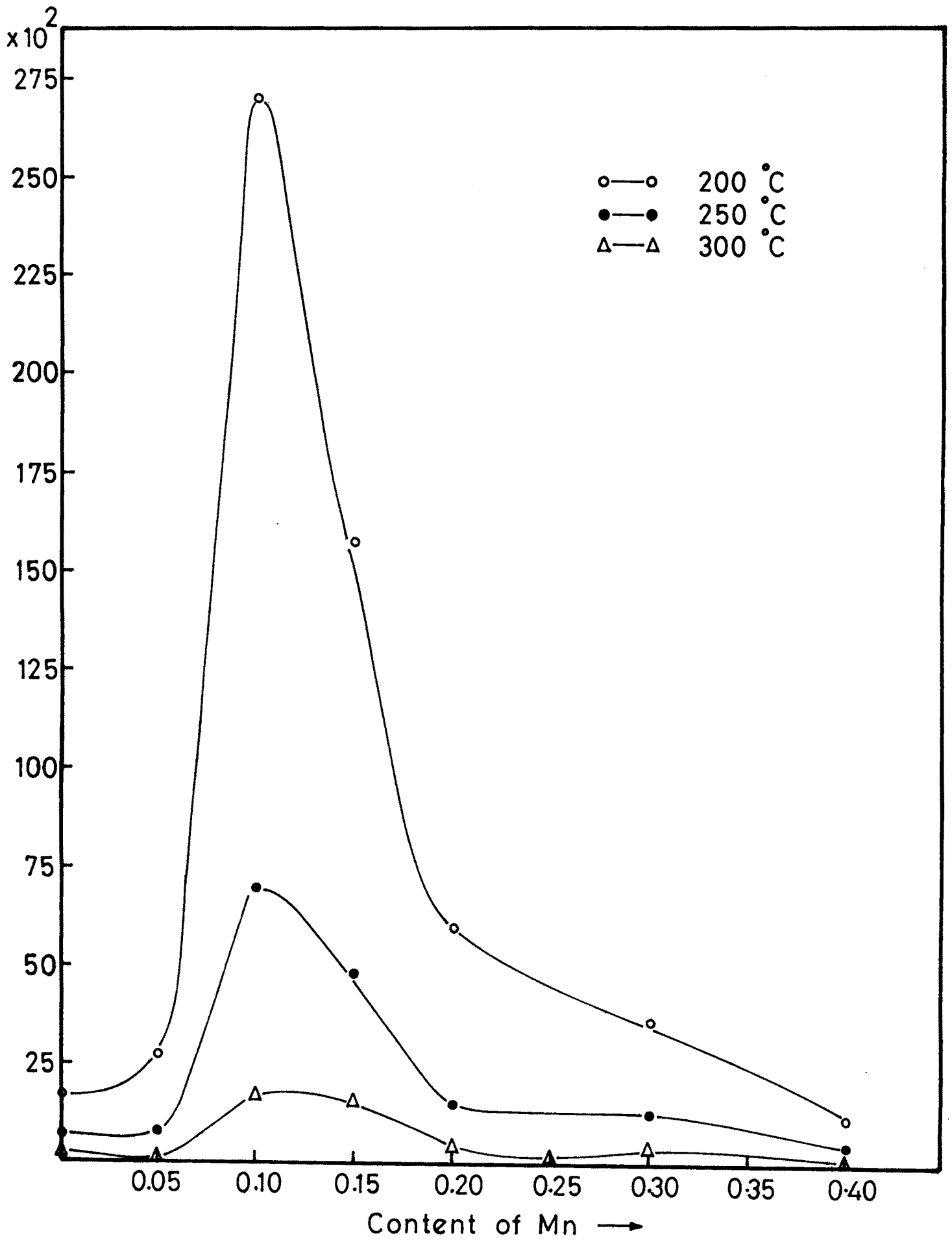


Fig. 4.7 - Variation of resistivity vs content of Mn.

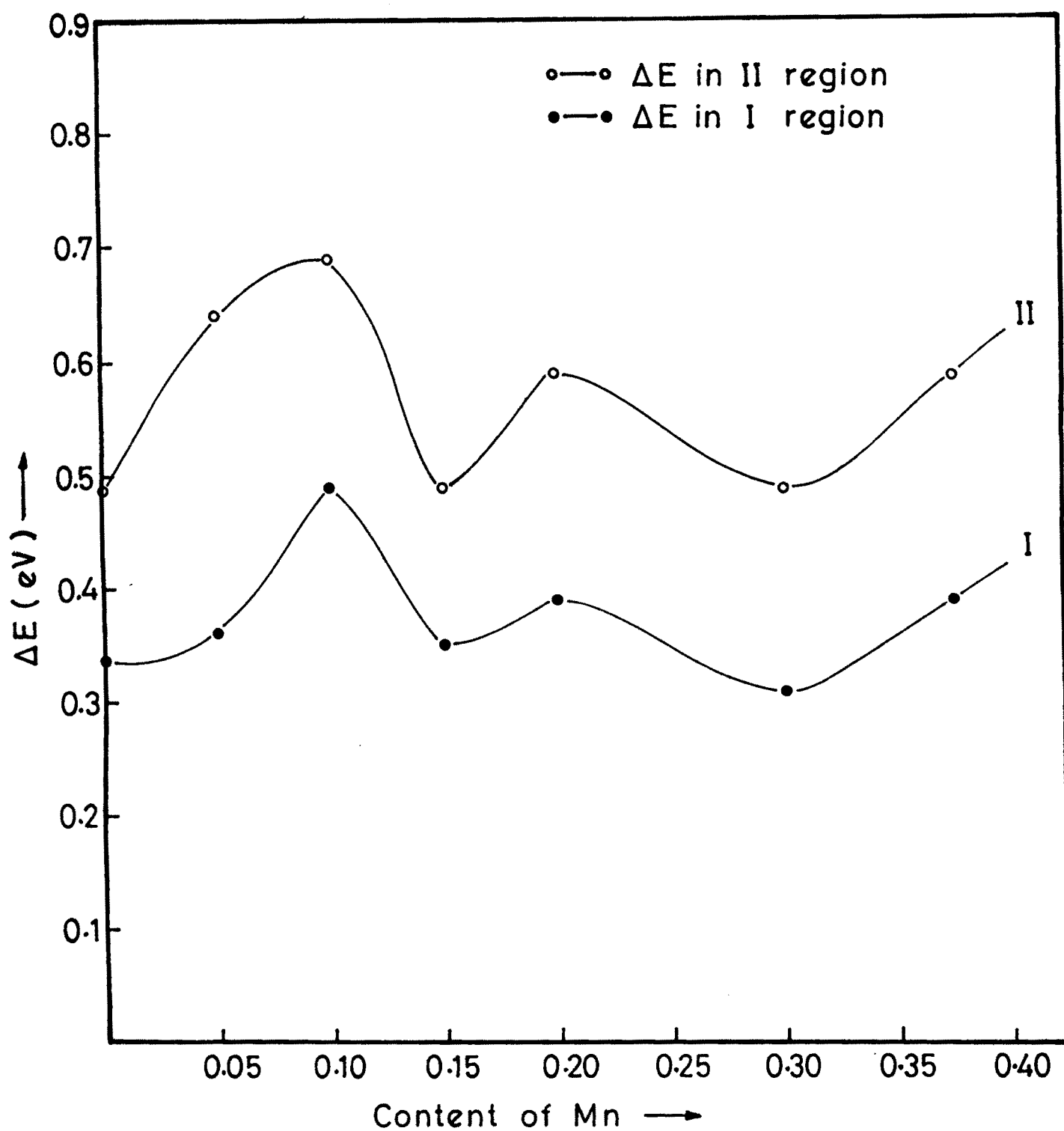


Fig. 4.8 - Variation of  $\Delta E$  vs content of Mn.



First transition temperature  $T_i$  increases with increase of Mn. This may be due to impurities or the formation of secondary phases at higher concentration of Mn. However, the resistivity also depends upon the following factors.

- i) Polycrystalline samples are sintered and contain pores. The pore probably air filled will be of a resistivity difference from that of the ferrite or garnet itself.
- ii) The grain size of individual crystallites in a polycrystalline sample can affect, among other things, the number of grain to grain contacts and thus influence the conduction paths and hence resistivity.
- iii) The chemical and / or heat treatment may results in chemical inhomogeneity. Thus with sintered rod there may be oxidation states on the outside of the rod different from those inside , again individual grains may be inhomogeneous for similar reason.<sup>39</sup>

#### 4.10(b) DIELECTRIC CONSTANT :

The observed room temperature values of  $\epsilon'$ ,  $\epsilon''$  and  $\tan\delta$  determined for the frequency of 10KHz are given in Table 4.2 together with the specimen composition.

From this it is seen that  $\epsilon'$ ,  $\epsilon''$  and  $\tan\delta$  decreases with increasing Mn concentration upto 0.15 and again increases. The D.C. conductivity also increases with increasing 'Mn' upto 0.15 and again decreases. Rezlescu and Rezlescu<sup>40</sup> studied the composition, frequency

TABLTABLE 4.2TABLE SHOWS VALUES OF  $\epsilon'$ ,  $\epsilon''$  AND  $\text{TAN}\delta$  AT 10KHz

Composition	$\epsilon'$	$\epsilon''$	$\text{TAN}\delta$
$\text{Cd}_{0.3}\text{Ni}_{0.7}\text{Fe}_2\text{O}_4$	127.64	131.34	1.029
$\text{Cd}_{0.3}\text{Ni}_{0.75}\text{Mn}_{0.05}\text{Fe}_{1.9}\text{O}_4$	122,59	134.85	1.100
$\text{Cd}_{0.3}\text{Ni}_{0.8}\text{Mn}_{0.1}\text{Fe}_{1.8}\text{O}_4$	25.46	7.012	0.2754
$\text{Cd}_{0.3}\text{Ni}_{0.85}\text{Mn}_{0.15}\text{Fe}_{1.7}\text{O}_4$	19.23	4.282	0.2227
$\text{Cd}_{0.3}\text{Ni}_{0.9}\text{Mn}_{0.2}\text{Fe}_{1.6}\text{O}_4$	29.72	16.15	0.5434
$\text{Cd}_{0.3}\text{Ni}_{1.0}\text{Mn}_{0.3}\text{Fe}_{1.4}\text{O}_4$	55.05	38.16	0.693
$\text{Cd}_{0.3}\text{Ni}_{1.1}\text{Mn}_{0.4}\text{Fe}_{1.2}\text{O}_4$	401.95	1145.56	2.85

and temperature dependance of 'Cu' containing mixed ferrites. V.R.K. Murthy and Jobhanadri<sup>41</sup> studied the dielectric properties of Ni-Zn ferrites. They explained the composition of dependance of dielectric constant by using the assumption that the mechanism of dielectric polarisation is similar to that of conduction.

According to Rabinkin and Novikova<sup>42</sup> the polarisation process in ferrite takes place through mechanism similar to conduction process. By

electronic exchange  $\text{Fe}^{3+} \rightleftharpoons \text{Fe}^{2+}$  one obtains local displacement of the electrons in the direction of the applied electric field, these displacement determine the polarisation. The decrease of polarisation with increasing frequency for spinel ferrites can be explained by the fact that, beyond a certain frequency of electric field the electronic exchange cannot follow the change in the direction of the field. The same interpretation was proposed by Reddy and Rao<sup>43</sup> for Ni substituted Li ferrites. A similar explanation can be given for the composition dependence of dielectric constant for present system  $\text{Cd}_{0.3}\text{Ni}_{0.7+t}\text{Mn}_t\text{Fe}_{2-2t}\text{O}_4$ . The electric conduction in Ni-Cd ferrites can be explained by the Verwey<sup>44</sup> mechanism. A number of such ions can be produced during sintering. It is known that a partial reduction of  $\text{Fe}^{3+}$  ions to  $\text{Fe}^{2+}$  ion can take place at higher temperatures. When the Ni containing ferrites are cooled from an elevated temperature in an oxidising atmosphere,  $\text{Ni}^{3+}$  ions are formed due to absorption of oxygen. The conduction takes place through electron exchange between  $\text{Ni}^{2+}$  and  $\text{Ni}^{3+}$  ions in the oxygen rich region and  $\text{Fe}^{2+}, \text{Fe}^{3+}$  ions in oxygen poor region.

The cation distribution for Mn substituted Ni-Cd ferrites is  $\text{Cd}_{0.3}\text{Fe}_{0.7}(\text{Ni}_{0.7}\text{Fe}_{1.3})$ . It is clear from the cation distribution given above that the iron concentration is maximum at octahedral site for the sample with  $t = 0$ , hence the number of  $\text{Fe}^{2+}$  ions on octahedral sites are more which take part in the electron exchange and hence are responsible for polarisation. Therefore a comparatively high value of dielectric constant is observed. The substitution of  $\text{Mn}^{4+}$  ion changes

the iron ion concentration from 2 to  $2-2t$  and Ni ion concentration from 0.7 to  $0.7+t$ , there by decreasing the number of ferrous ion on the octahedral sites which are available for polarisation with a consequent decrease in dielectric constant.  $Mn^{4+}$  ions present at B-site may localize  $Fe^{2+}$  ions by forming stable electrical bonds with  $Fe^{2+}$  ions. This localization effect obstructs the electron exchange interaction by reducing the effective number of free  $Fe^{2+}$  ions with a consequent decrease in the dielectric constant, with increasing 'Mn' concentration upto  $t = 0.15$ .

It is very probable that in the samples for  $t \geq 0.15$ , formation of  $Ni^{2+}$  to  $Ni^{3+}$  and  $Mn^{4+}$  to  $Mn^{3+}$  is possible. At higher compositions the formation of  $Mn_2O_3$  or  $Mn_3O_4$  is possible only at a higher temperatures such as  $4MnO_2 \xrightarrow{1000^\circ C} Mn_3O_4 + MnO_2 + O_2 \uparrow$ . These  $Mn^{3+}, Ni^{3+}$  ions preferentially occupy B-sites, so that conduction takes place through electron exchange between  $Ni^{2+} \& Ni^{3+}, Mn^{3+} \& Ni^{2+} Ni^{3+} Mn^{3+}$  ions. Therefore the decrease in resistivity agrees well with the assumption made by C.Prakash, J.S.Baijal<sup>45</sup>. Hence the dielectric constant again increases with increase of Mn content. The presence of single phase as established by X-ray diffraction pattern confirms the hypothesis that, the conduction mechanism in these ferrites is characteristics of single phase spinel structure rather than other phases. Thus the presence of Mn with multivalence state the unexplod nature of the ferrite grain, the excess presence of oxygen and the cluster formation of  $Mn_2O_3$  that leads to complex dielectric structure.<sup>46</sup>

The variation of dielectric constant with frequency for various compositions is given in Fig. 4.9. All these samples reveal dispersion

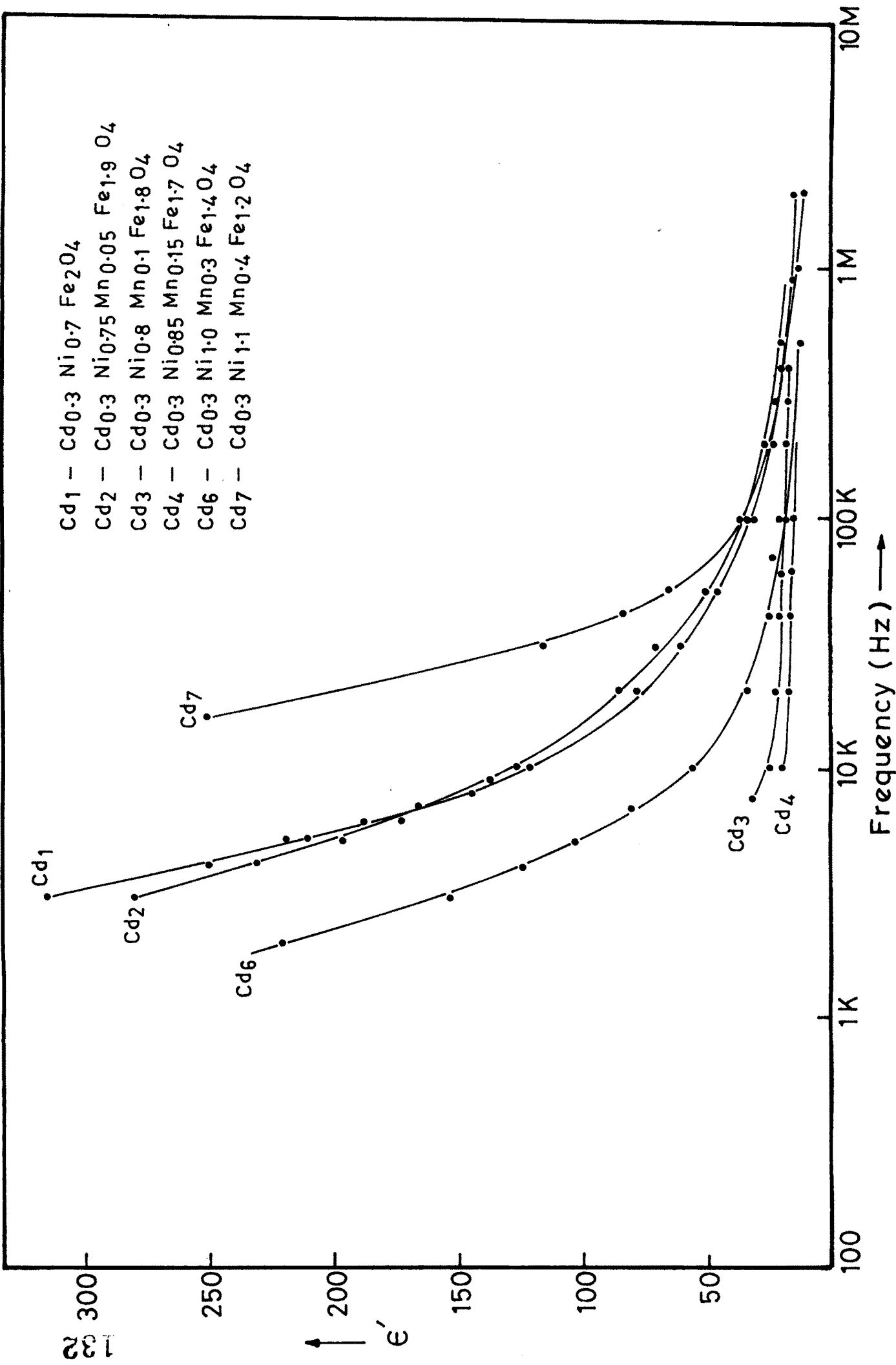


Fig. 4.9 - Variation of  $\epsilon'$  vs frequency.

due to Maxwell and Wagner interfacial polarisation in agreement with Koops phenomenological theory.

A comparison of dispersion curve for the samples with increase in Mn concentration shows that the change in the value of dielectric constant at lower frequencies of the applied field is larger than that at higher frequencies. The variation of dielectric relaxation intensity i.e. the difference between low and high frequency, dielectric constant with Mn concentration is therefore primarily governed by the change in the dielectric constant at low frequencies. The observed variation in dielectric relaxation intensity can be explained on the basis of space charge polarisation due to the inhomogeneous dielectric structure. The space charges polarisation is governed by number of space charge carriers and the resistivity of the sample.. The dielectric properties of ferrite materials are very sensitive to method of preparation, sintering temperature, sintering atmosphere and the amount and type of substitution. When the ferrite powder is sintered under slightly reducing conditions, the divalent iron ions are produced in the bulk of the material. These ions formed high conductivity grains separated by low conductivity layers and as a result the ferrite behaves as an inhomogeneous dielectric material.

The variation of  $\tan \delta$  with frequency for various compositions is shown in Fig. 4.10. All the compositions show a dispersion in  $\tan \delta$  with frequency. It is also observed that the loss tangent ( $\tan \delta$ ) goes on decreasing and again increasing in a similar way which is observed for dielectric constant with 'Mn' content. It can be concluded that for

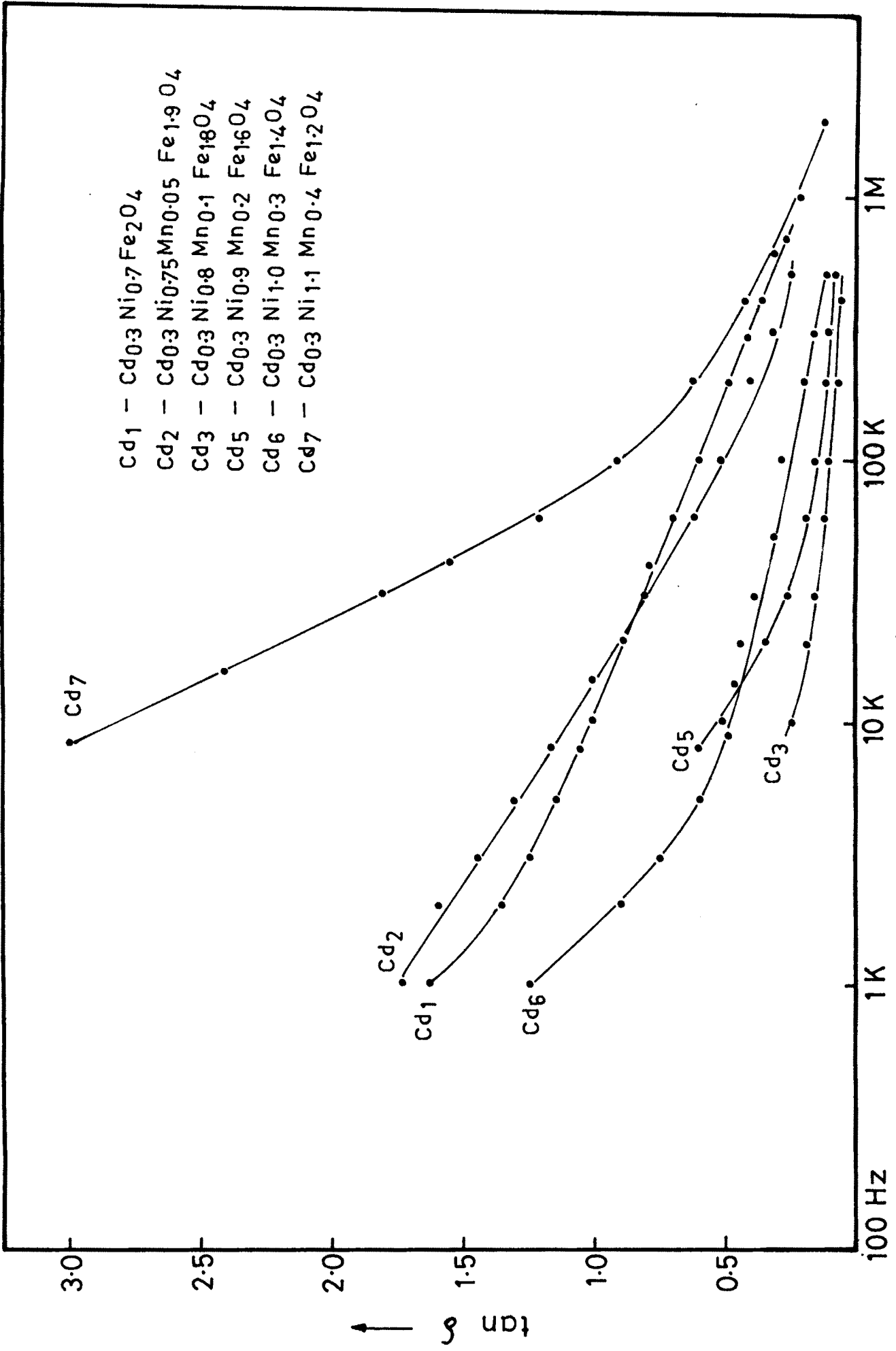


Fig. 4.10 - Variation of tan  $\delta$  with frequency.

for  $t < 0.15$ , the response of dielectric is dominated by  $Mn^{4+}$  with  $Ni^{2+}$  in usual manner, where as for  $t \geq 0.15$  the dielectric response is dominated by the complex nature of dielectric. The complex nature of dielectric may be due to the presence of Mn in the multivalence state. The unexplained nature of ferrite grains and the cluster formation of impurity phases. Thus the sample shows decrease and increase of dielectric constant with increasing Mn content.

## R E F E R E N C E S

1. Sooho R.E., ' The theory and application of ferrites' Pretic Hall Inc. New Jersey (1960).
2. Stuyts A.L. and Delau K.G., Sintering 7, 147 (1975).
3. Verwey E.J.W., Haayman, P.W., Romejn F.C., Van Costerhout G.w. Phillips Res.Rep. 5, 173 (1950).
4. A Broese Van Groenou, R.F. Bongera and A.L. Stuyts, Mater.Sci. Eng. 3, 317-392 (1968-69).
5. D.Condarache, Bull. Inst. Politich Isai I (Rumania). PP 103-6 (1974).
6. Komar A.P., Klivshin V.V., Bull. Sci. USSR Phy-18, P.96 (1954) (Columbia Univ. Techn. Translation).
7. Verwey E.S.W., Haayman P.W., Romejn F.C., Journal of Chem. Phys. 15, 181 (1947).
8. Romejin F.C., Phillips Res. Rep.8, 304 (1953).
9. Van Uitert L.G., Proc. Inst. Radio. Eng.44, 1294 (1956).
10. Koop's C.G., Phys. Rev. 83, 121 (1951).
11. M.I. Klinger, J.Phys. C. (G.B.) Vol.8, No.21. P. 3595-3607 (7th Nov. 1975)
12. M.I. Klinger, J.Phys. C.(G.B.) Vol.8, No. 21 P. 3595-3607 (7th Nov. 1975).
13. Kilnger M.I., Phy. State Solidi (B)79, 9 (1977).
14. Parker R., Tinsley C.J., Ferrites Proc. Int. Conf. Tokyo P-591 (1971).
15. Ahmed A.G., Miryasor N.Z., Fiz. Trer. Tela.(USSR)-13, 2759 (1971). Trans. Sort-Phy-Solid-State(USA).

16. Shrinivasan G., Phys. State, Solid(A) 55, P.K. 149 (1979).
17. Craik D.J., (Editor) Magnetic Oxides Part-1 P421 Wiley Interscience Publication (1975).
18. De-Boer J.H., Verwey E.J.W., Proc. Phys. Soc. 49, (extra Part) 59 (1937).
19. Jonker J.H., J.Phys. Chem. Solid 9, (1659).
20. Van Uitert L.G., Proc. Inst. Radio. Engrs. 44, 1249 (1956).
21. Koop's C.G., Phys. Rev. 83, 121 (1951).
22. Standley K.J., 'Oxide magnetic Material' 2nd edition Clarendon Press Oxford P.139, (1972).
23. Mott N.F., Gurney R.W., 'Electronic Processes in Ionic Crystals'. Oxford Uni. Press. (1948).
24. Frelich H., Adv. Phys. 3, 325 (1954).
25. Parker R., Phil. Mag. 3, 853 (1958).
26. Koop C.G., Phys. Rev. 83, 121 (1951).
27. Koops C.G., Phys. Rev. 83, 121 (1951).
28. Maxwell J.C., 'Electricity and Magnetism' Oxford Uni. Press, London Vol 11, 828 (1873).
29. Wagner K.w., Ann. Physik, 40, 817 (1913).
30. Bady I, and Collins T., Inst. Elect. Electron Engrs. Trans. Mic. Theory MTT-11, 222 (1963).
31. Brockman F.W., Dowling P.H. and Steneck W.G., Phys. Rev. 77, 85 (1950).
32. Komar A.P., Klivshin V. v., Bull. Acad. Sci., USSR Phys, 18, 96 (1954).

33. Verwey E.J.W., Haayman P.W., Romejn F.C., J.Chem. Phy.15, 181 (1947).
34. Ghani A. A., Etach A.I., Mohened A.A., Proc. ICF (1980),216.
35. Usha Varshney and R.J. Churchill, R.K. Puri and R.G. Mendiratta, ICF(5), IIT Bombay. India P.P. 255 (1989).
36. Jain G. G., Das B.K., Kumaris, J.App.Phys. 49, 2894, (1978).
37. C.d.Sabane, A.P.B. Sinha and A.B. Biswas, Ind. J.Pure. Appl. Phys. Vol-4, 187, (May 1966).
38. R.K.Puri, Vijay K. Babbar, R.G Mendiratta, Proc. ICF.5, 239 (1989).
39. Standley K.J., 'Oxide Magnetic Material,' 2nd edition Clarendon Press Oxford P.139, (1972).
40. N. Rezlescu and E Rezlescu, Phys. State Solidi (A) 23, 574 (1974).
41. V.R.K. Murthy and J.Sobhanadri, Phys. State.Solidi(A) 36,K-133, (1976).
42. L.I. Rabikin and Z.I. Novikova, Ferrites, Minsk P-146, 1960.
43. P.V.Reddy and T.S. Rao., J.Less-Common Met. 86, 255 (1982).
44. E.J.W. Verwey and J.H. de Boer, Red. Trav. Chim. Pays-Bas 55, 531 (1936).
45. Chandra Prakash and J.S. Baijal, J. of Less-common met.107, 51-57, (1985).
46. J.I. Powar, S.R.Sawant, S.A.Patil and R.N.Patil and R.N. Karekar., Mat. Res. Bull Vol-17, P.P. 339-343, (1982).